Acta Pharmacologica Sinica (2015) 36: 758–768
 1671-4083/15
www.nature.com/aps

Original Article

Fructus phyllanthi tannin fraction induces apoptosis and inhibits migration and invasion of human lung squamous carcinoma cells *in vitro* via MAPK/MMP pathways

Hai-juan ZHAO[1, 2], Ting LIU[1], Xin MAO[1, 2], Shu-xian HAN[1], Ri-xin LIANG[1], Lian-qiang HUI[1], Chun-yu CAO[1], Yun YOU[1, *], Lan-zhen ZHANG[2, *]

[1]*Institute of Chinese Materia Medica, China Academy of Chinese Medical Sciences, Beijing 100700, China;* [2]*School of Chinese Materia Medica, Beijing University of Chinese Medicine, Beijing 100102, China*

Aim: Fructus phyllanthi tannin fraction (PTF) from the traditional Tibetan medicine Fructus phyllanthi has been found to inhibit lung and liver carcinoma in mice. In this study we investigated the anticancer mechanisms of PTF in human lung squamous carcinoma cells *in vitro*.

Methods: Human lung squamous carcinoma cell line (NCI-H1703), human large-cell lung cancer cell line (NCI-H460), human lung adenocarcinoma cell line (A549) and human fibrosarcoma cell line (HT1080) were tested. Cell viability was detected with MTT assay. Cell migration and invasion were assessed using a wound healing assay and a transwell chemotaxis chambers assay, respectively. Cell apoptosis was analyzed with flow cytometric analysis. The levels of apoptosis-related and metastasis-related proteins were detected by Western blot and immunofluorescence.

Results: PTF dose-dependently inhibited the viability of the 3 human lung cancer cells. The IC_{50} values of PTF in inhibition of NCI-H1703, NCI-H460, and A549 cells were 33, 203, and 94 mg/L, respectively. PTF (15, 30, and 60 mg/L) dose-dependently induced apoptosis of NCI-H1703 cells. Treatment of NCI-H1703 and HT1080 cells with PTF significantly inhibited cell migration, and reduced the number of invasive cells through Matrigel. Furthermore, PTF dose-dependently down-regulated the expression of phosphor-ERK1/2, MMP-2, and MMP-9, up-regulated the expression of phosphor-JNK, but had no significant effect on the expression of ERK1/2 or JNK.

Conclusion: PTF induces cell apoptosis and inhibits the migration and invasion of NCI-H1703 cells by decreasing MPPs expression through regulation of the MAPK pathway.

Keywords: *Phyllanthus emblica* L; tannins; lung squamous carcinoma; apoptosis; metastasis; MAPK; MMPs

Acta Pharmacologica Sinica (2015) 36: 758–768; doi: 10.1038/aps.2014.130; published online 13 Apr 2015

Introduction

Lung cancer is the leading cause of cancer related deaths, and 80% of lung cancer cases are non-small cell lung cancer (NSCLC)[1]. Squamous cell carcinoma and adenocarcinoma are two major histological subtypes of NSCLC. Although tobacco smoking increases the risks of all major histological subtypes of lung cancer, it appears to be a stronger risk factor for squamous cell carcinoma than for adenocarcinoma[2, 3]. Because the population of smokers is rapidly growing, chemopreventive and therapeutic agents for NSCLC are urgently needed.

The malignancy in NSCLC is often attributed to its invasive and metastatic abilities, and distant metastasis is one of the main reasons for the poor prognosis of lung cancer patients[4]. A chemotherapeutic agent that possesses the ability to induce apoptosis and inhibit migration or invasion might be more effective. Studies have demonstrated that molecules that drive the dissemination of malignant cells are shared among cancers, and drugs that inhibit metastasis are broadly beneficial[5]. Apoptotic regulators often contribute to cell metastasis[6]. Accumulating evidence indicates that mitogen-activated protein kinases (MAPKs) play a major role in apoptosis signaling. MAPKs belong to an evolutionarily conserved and ubiquitous signal transduction superfamily of Ser/Thr protein kinases,

* To whom correspondence should be addressed.
E-mail youyunrice@126.com (Yun YOU);
zhanglanzhen01@126.com (Lan-zhen ZHANG)
Received 2014-07-28 Accepted 2014-10-30

and this superfamily participates in malignant tumor genesis, invasion, and metastasis through the regulation of cellular apoptosis[7, 8]. Persistent activation of extracellular signal-regulated kinase (ERK) in malignant cells can lead to an enhanced induction of matrix metalloproteinases (MMPs), as well as extracellular matrix and basement-membrane degradation, which enable the cancer cells to invade surrounding tissues[7].

Fructus phyllanthi, the dried ripened fruit of *Phyllanthus emblica* L and a traditional Tibetan medicine, has been used clinically for thousands of years in the Tibetan area. Its active extracts have been shown to possess several pharmacologic activities, including anti-tumor, anti-inflammatory, anti-bacterial, and anti-viral activities[9–11]. Fructus phyllanthi primarily contains tannins, phenolic compounds, phyllembelic acid, rutin, curcuminoids, and emblicol[12]. Previous reports have demonstrated that the juice of fructus phyllanthi can inhibit the formation of N-nitrosomorpholine *in vitro* and *in vivo* with an inhibition rate greater than 90%[13]. The juice has been shown to distinctly inhibit the proliferation of S-180 and H-22 cells in transplanted mouse tumors and to protect somatic and germ cells from DNA damage[14]. Our previous studies have demonstrated that the fructus phyllanthi tannin fraction (PTF) could significantly inhibit Lewis lung carcinoma and H-22 liver carcinoma proliferation in mice (data not shown) .

The objective of this study was to assess the anti-metastatic activity of PTF in a lung squamous cell carcinoma cell line (NCI-H1703). The cytotoxic effects of the PTF on cancer cell lines were thoroughly screened to select a non-toxic effective dose. Our second objective was to investigate the potential molecular mechanisms underlying the metastasis inhibition and the apoptosis induction of PTF through MAPK and MMP pathways.

Materials and methods

Materials

The human lung adenocarcinoma cell line (A549), human large-cell lung cancer cell line (NCI-H460), human lung squamous carcinoma cell line (NCI-H1703), and human fibrosarcoma cell line (HT1080) were obtained from the Institute of Basic Medical Sciences, Chinese Academy of Medical Sciences (Beijing, China).

Fructus phyllanthi herbs grown in Nepal were purchased from the Beijing Tibetan Hospital. Etoposide was purchased from Qilu Pharmaceuticals Ltd (Ji'nan, China). Procaspase-activating compound 1 (PAC-1) was purchased from Bio Vision (San Francisco, CA, USA). RPMI 1640 medium, Modified Eagle's Medium (MEM), and trypsin were purchased from Hyclone (Logan, UT, USA). Fetal bovine serum (FBS), methyl thiazolyl tetrazolium (MTT), penicillin, and streptomycin were purchased from GIBCO (San Diego, CA, USA). Matrigel was purchased from Becton-Dickinson Biosciences (San Diego, CA, USA). Ninety-six- and 24-well culture plates and a 24-well transwell chemotaxis chamber were obtained from Costar (Cambridge, MA, USA). Rabbit polyclonal anti-JNK was purchased from Santa Cruz Biotechnology (Santa Cruz, CA, USA). Purified mouse monoclonal anti-phospho-JNK, rabbit monoclonal anti-phospho-ERK1/2 and anti-MMP-9 were purchased from Cell Signaling (Danvers, MA, USA). Mouse monoclonal anti-MMP-2 was purchased from Abcam (Cambridge, MA, USA). The rabbit polyclonal anti-ERK1/2, mouse monoclonal anti-β-actin, goat anti-mouse IgG, goat anti-rabbit IgG antibodies, a BCA protein assay kit, and an enhanced chemiluminescent method of Western blotting assay kit were purchased from Boster (Wuhan, China). The annexin V-FITC/PI apoptosis assay kit, Giemsa, and phosphate-buffered saline (PBS) were purchased from Solarbio (Beijing, China). The polyvinylidene fluoride (PVDF) membranes were purchased from Millipore (Bedford, MA, USA). The protease inhibitor cocktail, phenylmethanesulfonyl fluoride (PMSF), and the other chemicals and reagents were obtained from Sigma (San Francisco, CA, USA). All chemicals and reagents were of analytical grade.

Preparation of PTF

A tungsten molybdophosphate-casein colorimetric method was used for the determination of the tannin level in the medical material of *Phyllanthus emblica* L with gallic acid as a reference substance, according to the method described by the Pharmacopoeia of China. The content of total tannins was greater than 56% in the PTF. The HPLC fingerprint of the PTF was established at 260 nm. Four main peaks were identified as chebulagic acid, gallic acid, corilagin, and ellagic acid (Figure 1). The HPLC fingerprint based quality evaluation of the PTF has been previously published[15].

The RP-HPLC method was used to quantify three representative constituents of the PTF, including gallic acid, corilagin, and ellagic acid. The concentrations of gallic acid, corilagin, and ellagic acid were 7.72%±0.06%, 1.87%±0.05%, and 3.67%±0.04%, respectively.

The purified PTF was dissolved in DMSO and subsequently diluted with RPMI-1640 medium or MEM medium to a final concentration.

Cell culture

A549, NCI-H460, and NCI-H1703 were grown in RPMI-1640 medium supplemented with 10% FBS, 100 U/mL penicillin, and 100 U/mL streptomycin. HT1080 was grown in MEM medium supplemented with 10% FBS, 100 U/mL penicillin, and 100 U/mL streptomycin. The cells were maintained in a tissue culture incubator at 37℃ in humidified air that contained 5% CO_2 until 80% confluence and then they were subcultured twice weekly.

Cytotoxic assay

To determine the cytotoxic effects of the PTF on the *in vitro* proliferative capabilities of the three lung cancer cell lines, A549, NCI-H1703, and NCI-H460, we performed the assay using MTT as previously described[16]. During the logarithmic growth phase, the cells were collected and seeded in 96-well tissue culture plates at a density of 1×10^4 cells/well in serum-containing medium and grown to 80% confluence. The cells were subsequently treated with the PTF at increasing concen-

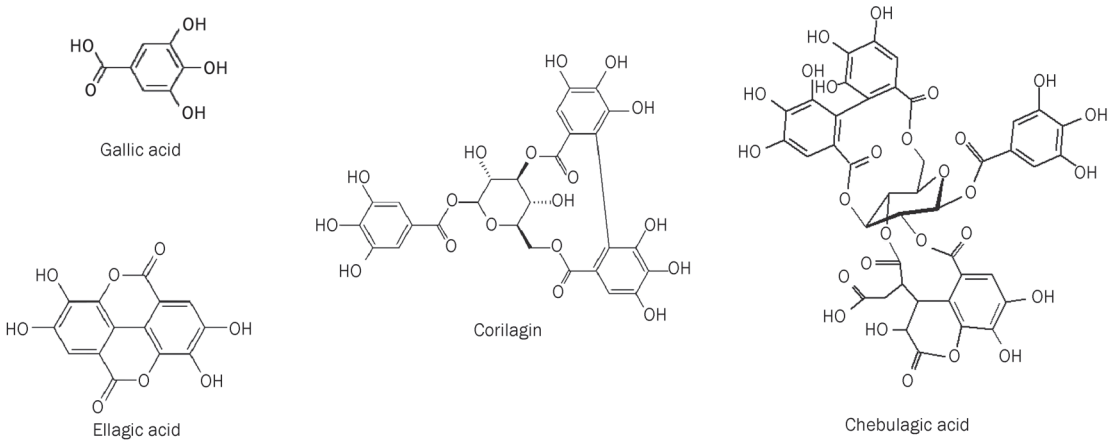

Figure 1. Chemical structures of gallic acid, ellagic acid, corilagin, and chebulagic acid, four main components in PTF.

trations of 31.2, 62.5, 125.0, 250.0, and 500.0 mg/L, and the same volume of DMSO was used as the vehicle control for the PTF experiments at a final concentration of 0.1%. After 48-h incubation, the cells were washed twice with PBS, and 200 μL of culture medium that contained 500 mg/L of MTT was added to each well and incubated for 4 h at 37°C. Finally, the culture medium was removed, and the formazan salt crystals were dissolved with 150 μL DMSO and shaken for 10 min. The absorbance was read at a wavelength of 570 nm using a Spectra Max M5 Microplate Reader (Molecular Devices, Sunnyvale, CA, USA). The results represent the averages of five parallel samples, and each sample was assayed in triplicate. The cell inhibitory rate was calculated as follows: inhibitory rate (%)=($A_{570\ control}$–$A_{570\ sample}$)/($A_{570\ control}$–$A_{570\ blank}$)×100%.

Cell migration assay

To determine the effects of the PTF on the migration of NCI-H1703 and HT1080 cells *in vitro*, the cells were seeded at a density of 2×10^5 cells/mL in 24-well tissue culture plates and cultured in medium containing 10% FBS to 90% confluence after 24 h. The medium was removed, and the cell monolayers were wounded by the manual scraping of the cells with a 20-μL plastic pipette tip. Debris was removed from the culture by washing twice with PBS, and the NCI-H1703 cells were then treated with fresh medium with 2% FBS that contained different concentrations of the PTF (7.5 or 15.0 mg/L) for 24 and 48 h. The HT1080 cells were treated with fresh medium with 2% FBS that contained different concentrations of the PTF (25.0, 50.0, and 100.0 mg/L) for 3, 6, and 9 h, respectively. Images were captured immediately after wounding at different time points with a Nikon Ti inverted microscope (Nikon, Tokyo, Japan). The migration area was measured using Bioflux Montage analysis software (Fluxion Bioscience Inc, South San Francisco, CA, USA). The migration area and migration inhibitory rate were calculated using the following formula: migration area=migration area after treatment–migration area at the beginning (mm^2); migration inhibitory rate=(average migration area of the control group–average migration area of the treatment group)/average migration area of the control group×100%. The experiments were repeated in triplicate wells at least three times.

Cell invasion assay

Cell invasion is a crucial process in tumor metastasis. A transwell chemotaxis chamber assay was performed to determine the ability of NCI-H1703 cells to invade biological matrices *in vitro*, which was based on the percentage of cells that penetrated the reconstituted basement membrane-coated filter and attached to its lower surface. For the cell invasion assay, the NCI-H1703 and HT1080 cells were treated with various concentrations of the PTF for 48 h; the cells were subsequently harvested and their *in vitro* invasiveness was determined using a 24-well transwell chemotaxis chamber. The filter surfaces (8-μm pore size) were coated with 30 μL of Matrigel at a uniform thickness for 1 h at 37°C. The treated cells were then seeded into the upper chamber at 2.5×10^4 cells/well in 100 μL of serum-free medium, and 700 μL of medium containing 10% FBS was added to the lower chamber as a chemo-attractant. After incubation for 24 h at 37°C and 5% CO_2, the filter was gently removed from the chamber. The remaining cancer cells on the upper surface of the filter were wiped off with a cotton swab. The cells that had invaded the lower surface of the filter were fixed with methanol and stained with Giemsa stain. The invasive cells attached to the lower side of the membrane were quantitatively assessed and expressed as the mean number of cells in four random fields (×200) per filter using a light microscope. The experiments were independently performed three times.

Flow cytometric analysis

To assess the mechanism underlying PTF-mediated growth inhibition, NCI-H1703 cells were treated with varying concentrations of the PTF (15.0, 30.0, and 60.0 mg/L) for 24 h, and the control group was treated with the same amount of vehicle

medium. PAC-1, an apoptosis inducer, was used as a positive control. Flow cytometric analysis was subsequently performed to detect apoptosis using an annexin V-FITC/PI apoptosis assay kit. According to the kit instructions, the adherent cells were collected by centrifugation at 111×*g* for 10 min. After two washes with cold PBS, the cells were resuspended at a density of 1×10^6 cells/mL. Two hundred micro-liter of binding buffer, 10 μL of annexin V-FITC, and 10 μL of PI were added to these cells, and they were incubated for 15 min at room temperature in the dark. Finally, the samples were analyzed using a flow cytometer (BD, San Diego, CA, USA).

Western blot analysis

Cells were incubated with varying concentrations of the PTF (15.0, 30.0, and 60.0 mg/L) for 24 h, the adherent cells were subsequently harvested, washed twice with ice-cold PBS, and lysed in RIPA buffer containing proteinase inhibitors (1% cocktail and 1 mmol/L PMSF) at 4 °C for 30 min. After centrifugation for 10 min at 10000×*g* at 4 °C, the protein concentration in the supernatant was determined with a BCA assay kit according to the manufacturer's instruction. Equivalent amounts of proteins (100 μg/lane) were separated by 10% sodium dodecyl sulfate polyacrylamide gel electrophoresis (SDS-PAGE) and subsequently transferred to PVDF membranes. Each membrane was blocked with 5% skim milk in Tris Buffered Saline with Tween-20 (TBST) saline (20 mmol/L Tris-HCl, pH 7.5, 137 mmol/L NaCl, and 0.1% Tween 20) at room temperature for 2 h and then incubated with the indicated primary antibodies against ERK1/2, p-ERK1/2, JNK, p-JNK, MMP-2, MMP-9, and β-actin overnight at 4 °C. After being washed with TBST, the membranes were incubated with secondary antibodies (HRP-conjugated goat anti-rabbit or goat anti-mouse IgG) for 2 h at room temperature and visualized with an enhanced chemiluminescence (ECL) detection system (Syngene, Cambridge, UK). The mean density of each band was analyzed using Bioflux Montage software (Fluxion Biosciences Inc, South San Francisco, CA, USA).

Immunofluorescence staining

The NCI-H1703 cells (4×10^4 cells/well) at the exponential phase of growth were seeded on glass coverslips in 6-well plates. The cells were allowed to adhere overnight, and the medium was subsequently removed and replaced with fully supplemented media containing different concentrations of the PTF (0, 15.0, 30.0, and 60.0 mg/L). After 24 h, the cells were rinsed with PBS and fixed using 4.0% paraformaldehyde for 15 min at room temperature. The cells were permeabilized with 0.1% Triton X-100 and blocked with normal serum blocking buffer at room temperature. Next, they were incubated with an antibody against MMP-2 (diluted 1:100) or anti-MMP-9 (diluted 1:800) at 4 °C overnight. The cells were incubated with an FITC-conjugated secondary antibody (diluted 1:100) in the dark. Then, they were rinsed three times and mounted using 50% glycerinum in PBS. Finally, the cells were examined using a Nikon Ti fluorescent microscope (Nikon, Tokyo, Japan).

Statistical analysis

Statistical analysis was conducted with SPSS v17.0 software (IBM Corporation, Armonk, NY, USA). All data are expressed as the mean±SD. Statistical analysis were performed using one-way analysis of variance (ANOVA) or Student's *t*-test. A *P*-value<0.05 was considered significant.

Results

Effects of PTF on the viabilities of the lung cancer cell lines NCI-H1703, NCI-H460, and A549

The effects of the PTF on the viabilities of the lung cancer cell lines were assessed using an MTT assay. The proliferative abilities of the cells were inhibited by PTF in a dose-dependent manner (Table 1). The 50% inhibitory concentrations (IC_{50}) of the PTF on NCI-H1703, NCI-H460, and A549 were 33.0, 203.0, and 94.0 mg/L, respectively, for 48 h, indicating that NCI-H1703 was substantially more sensitive to the PTF, therefore, we chose these cells for the subsequent experiments.

Table 1. Inhibition rate of PTF on NCI-H1703, NCI-H460, and A549 cells viability (%) (mean±SD, *n*=15). $^bP<0.05$, $^cP<0.01$ *vs* vehicle control group.

Groups	Dose	NCI-H1703	NCI-H460	A549
Control	0	–	–	–
PTF	31.2 mg/L	33.6±5.6^c	4.3±1.2	16.9±2.8^c
	62.5 mg/L	99.3±0.4^c	10.5±2.8^b	42.9±1.8^c
	125.0 mg/L	99.5±0.1^c	18.7±4.2^c	49.1±1.7^c
	250.0 mg/L	99.2±0.2^c	48.9±5.0^c	44.6±1.5^c
	500.0 mg/L	98.7±0.4^c	53.2±6.8^c	65.1±5.4^c
Etoposide	10 μmol/L	86.2±1.4^c	69.7±3.7^c	76.3±0.6^c

Effects of PTF on migration of NCI-H1703 and HT1080

The results indicated the time- and dose-dependent effect of the clear reduction in the NCI-H1703 cell migration following treatment with the PTF. Exposure to the PFT for 48 h induced significant decreases in the NCI-H1703 cell migration area (Figure 2A) and an increase in the inhibition rate of these cells (Figure 2C) compared with the cells exposed to the PTF for 24 h ($P<0.001$). Because the NCI-H1703 cell migration ability was lower, highly metastatic human fibrosarcoma cells (HT1080) were selected for migration and invasion experiments to confirm the effects of the PTF on tumor metastasis.

The effects of the PTF on the cell proliferation activity of HT1080 were detected via an MTT assay, which showed that its IC_{50} was 274.0 mg/L. The non-toxic doses of the PTF (25.0, 50.0, and 100.0 mg/L) were subsequently selected for the migration and invasion study. A time- and dose-dependent decrease in the migration area of HT1080 was identified. The PTF at a concentration of 100.0 mg/L significantly inhibited ($P<0.001$) the spread of the HT1080 cells along the edges of the wound after a 3-h treatment compared with the untreated control cells (Figures 2B and 2D).

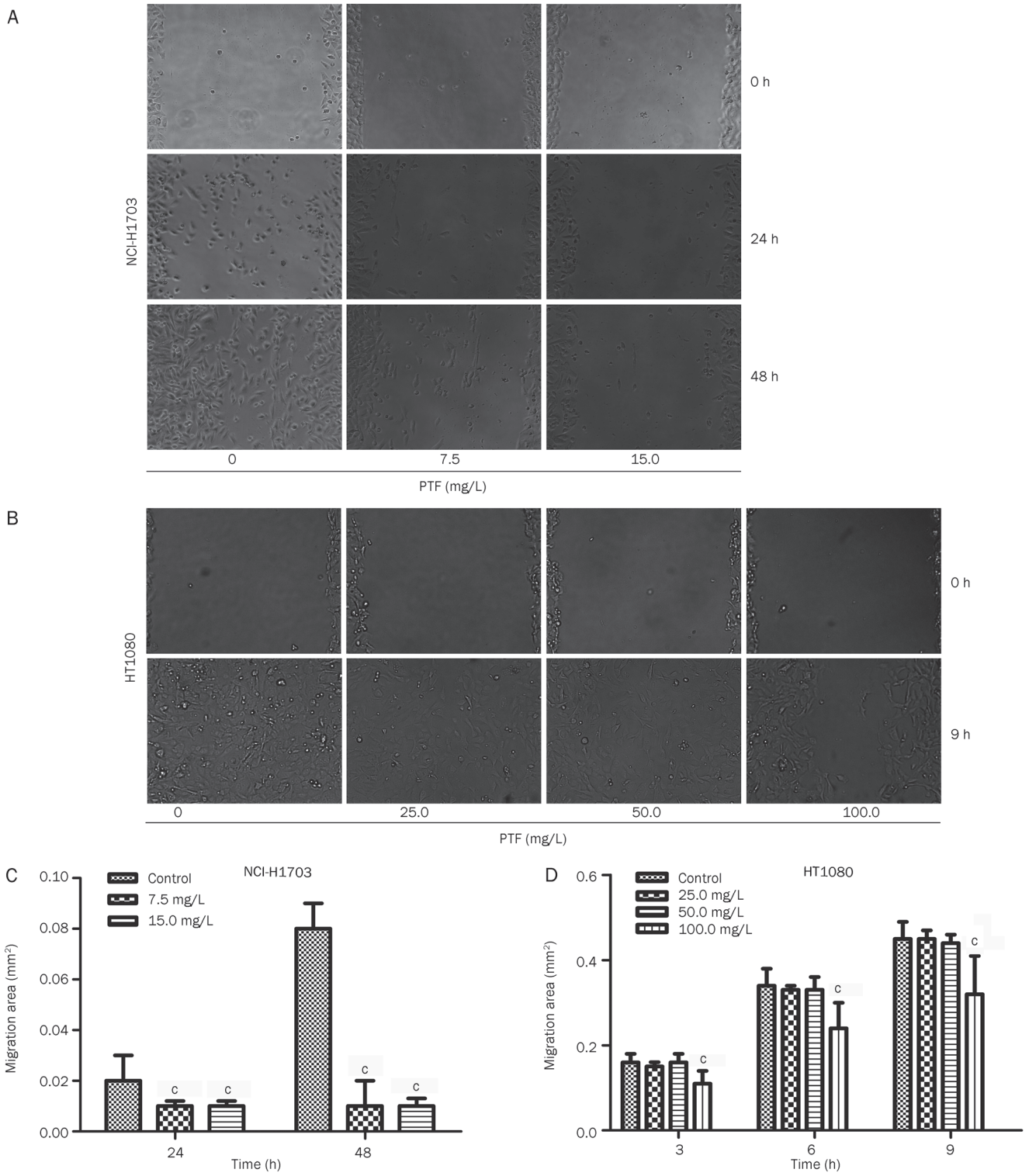

Figure 2. Inhibitory effects of PTF on the migration of NCI-H1703 and HT1080 cells *in vitro*. The confluent NCI-H1703 and HT1080 monolayers were wounded by scraping; NCI-H1703 were subsequently treated with PTF at a dose of 7.5 or 15.0 mg/L, whereas HT1080 were treated with PTF at a dose of 25.5, 50.0, or 100.0 mg/L. (A) PTF inhibited NCI-H1703 cell migration to the wound surface was monitored at different time points. (B) PTF inhibited HT1080 cell migration (magnification ×200). (C) and (D) The migratory areas were measured and analyzed using Bioflux Montage software for NCI-H1703 and HT1080 respectively. Mean±SD. n=5. ^{c}P<0.01 *vs* the control group.

Effects of PTF on the invasion of NCI-H1703 and HT1080

The invasion capacities of the NCI-H1703 and HT1080 cells were significantly inhibited ($P<0.001$, $P<0.05$) by the PTF (Figure 3A), the number of invasive cells decreased when the PTF concentration increased (Figure 3B). Reductions of approximately 29% and 61% were observed for the NCI-H1703 cells 48 h after the treatment with 7.5 and 15.0 mg/L of the PTF compared with the control, respectively. Forty-eight hours after the treatment with different concentrations of PTF (25.0, 50.0, and 100.0 mg/L) reduced the invasion of HT1080 cells by 24%, 47%, and 69%, respectively. These results indicated that the PTF inhibited the invasion of NCI-H1703 and HT1080 cells and inhibition in a dose-dependent manner.

Effects of PTF on apoptosis of NCI-H1703

Compared with the control, the cells in the PTF-treated group exhibited obvious morphological features associated with apoptosis, including shrinkage of the cytoplasm, plasma membrane blebbing, and cellular decomposition into membrane-bound apoptotic bodies (Figure 4A).

The inhibition of cell viability might have resulted from the induction of apoptosis. The flow cytometric results indicated that the PTF induced dose-dependent apoptosis at both the early and late stages (Figure 4B), mainly during early apoptosis (Figure 4C). The NCI-H1703 cells were treated with 15.0, 30.0, or 60.0 mg/L of PTF for 24 h exhibiting early apoptosis rates of 12.41%±3.72%, 14.8%±3.92%, and 17.85%±8.60%, respectively, which were substantially and significantly different from the vehicle control. The results demonstrated that the PTF partially inhibited the viability of the NCI-H1703 cells through the induction of apoptosis.

Effects of PTF on expression of ERK1/2 and JNK MAPK signaling pathways in NCI-H1703

Statistical calculation of the p-ERK/ERK and p-JNK/JNK expression ratios indicated that treatment with the PTF

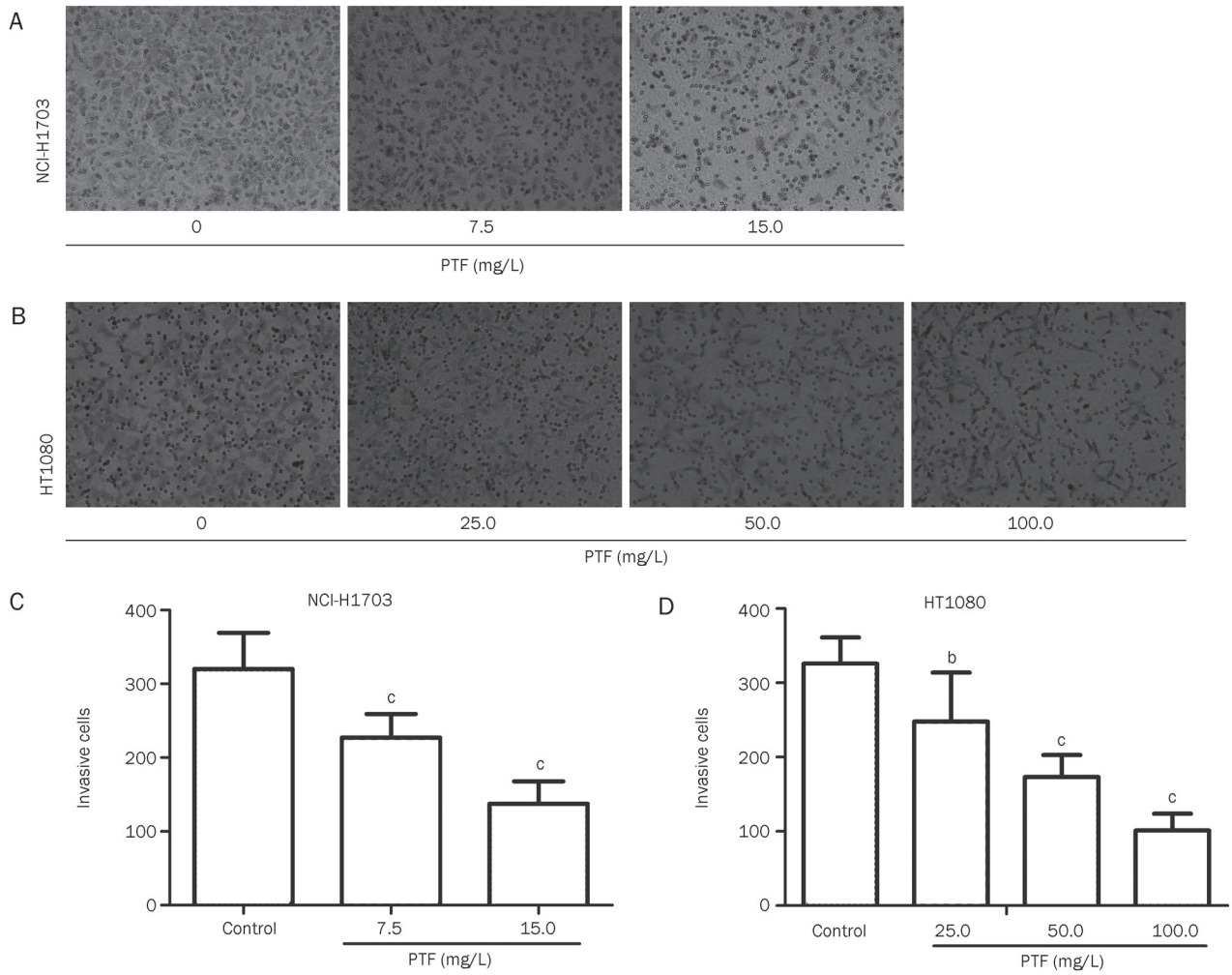

Figure 3. Inhibitory effects of PTF on the invasion of NCI-H1703 and HT1080 cells. NCI-H1703 were treated with PTF at a dose of 7.5 or 15.0 mg/L, and HT1080 were treated with PTF at a dose of 25.5, 50.0, or 100.0 mg/L. Forty-eight hours later, the cells were harvested and seeded into the upper chamber coated with Matrigel. The number of cells that invaded the lower chamber represented the invasion capabilities. (A) PTF inhibited NCI-H1703 cells invasion, and (B) PTF inhibited HT1080 cell invasion (magnification ×200). (C) and (D) Quantification of the invaded NCI-H1703 and HT1080 cells. Mean±SD. $n=6$. $^bP<0.05$, $^cP<0.01$ *vs* the control group.

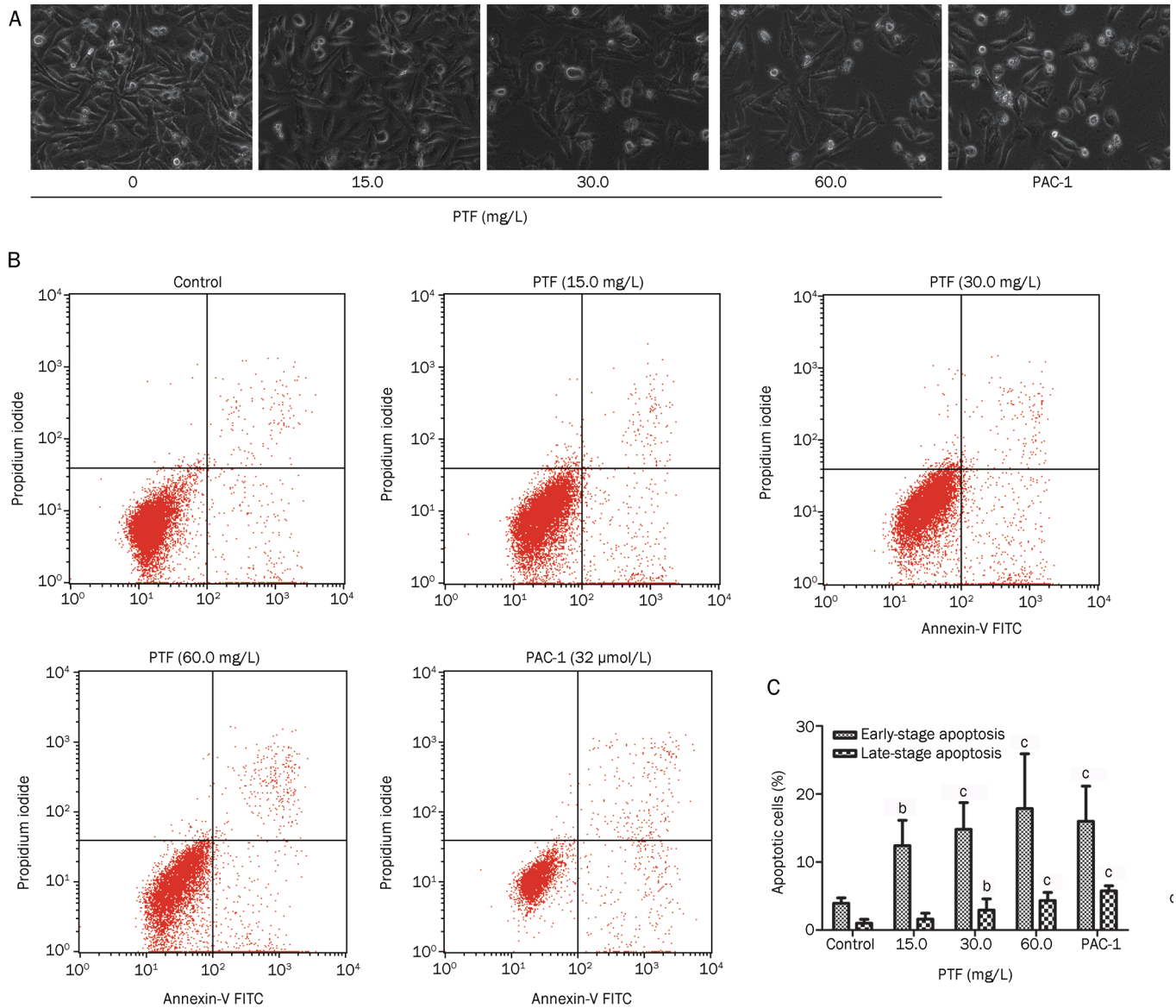

Figure 4. The effects of PTF on apoptosis induction in NCI-H1703 cells. (A) NCI-H1703 cells were exposed to PTF at a dose of 15.0, 30.0, or 60.0 mg/L and the procaspase-activating compound 1 (PAC-1, 32 μmol/L) for 24 h. Apoptotic morphological changes, such as cytoplasm shrinkage and plasma membrane blebbing, were observed using a light microscope (×200). (B) NCI-H1703 cells were treated with different doses of PTF in complete culture medium for 24 h, and apoptosis was measured by annexin-V and propidium iodide staining followed by flow cytometry detection. Three populations of cells were observed: viable cells (negatively stained, lower left quadrants), early apoptotic cells (annexin-V positive and propidium iodide negative, lower right quadrant) and cells in the late stages of apoptosis (annexin-V and propidium iodide positive, upper right quadrants). (C) Quantitative analysis of early and late apoptosis in NCI-H1703 cells induced by different doses of PTF. The data are provided as the mean±SD. n=4. ^{b}P<0.05, ^{c}P<0.01 *vs* the control.

decreased the p-ERK1/2 level and increased the p-JNK level (Figure 5A). As shown in Figure 5B, the ratio of p-ERK/ERK was significantly reduced by 50.3% in the 60.0 mg/L PTF group compared with the vehicle control (P<0.01). The p-JNK expression was increased, and the ratio of p-JNK/JNK was significantly increased by 23.0% in the 60.0 mg/L PTF group compared with the vehicle control (P<0.01). In parallel, the PTF had no significant effects on the expression of ERK1/2 or JNK. The results suggested that the MAPK signaling pathway was involved in the apoptosis-inducing effect of the PTF.

Effects of PTF on expression of MMP-2 and MMP-9 in NCI-H1703

To elucidate the potential underlying mechanisms of the anti-metastatic activities of the PTF on NCI-H1703 cells, we detected changes in MMP-2 and MMP-9 expression via Western blot and immunofluorescence staining. As shown in Figure 6A, the Western blots indicated that the PTF treatment significantly decreased the expression of MMP-2 and

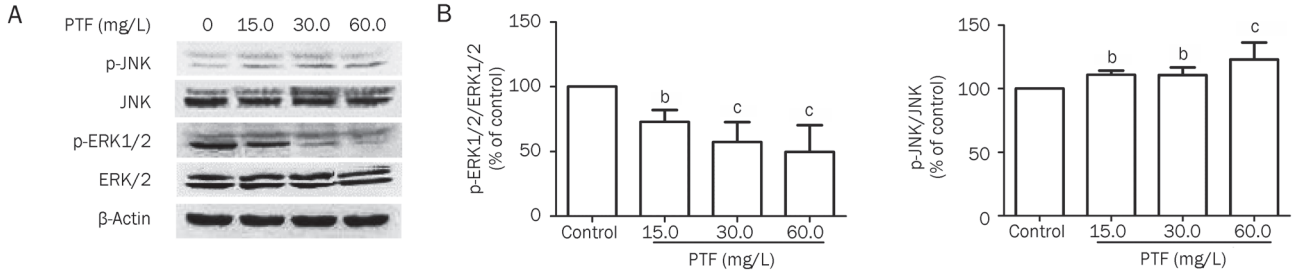

Figure 5. The effects of PTF on ERK1/2 and JNK expression in NCI-H1703 cells. (A) Total expression and phosphorylation of ERK and JNK were analyzed by Western blotting in NCI-H1703 cells treated with PTF for 24 h. β-Actin was used as a loading control. (B) The ratios of p-ERK/ERK and p-JNK/JNK were analyzed. Results are represented as the mean±SD from three independent experiments. n=3. ^bP<0.05, ^cP<0.01 *vs* the control.

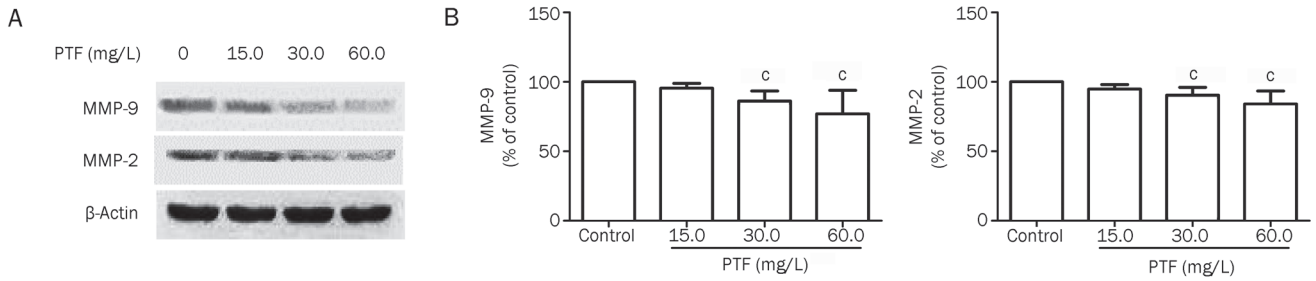

Figure 6. Inhibitory effects of PTF on MMP-2 and MMP-9 expression in NCI-H1703 cells. (A) Changes in the protein expression of metalloproteinases MMP-9 and MMP-2 in NCI-H1703 treated by PTF. β-Actin was used as a loading control. (B) PTF decreased MMP-2 and MMP-9 expression in NCI-H1703 cells, which was assessed via quantitative densitometry analysis. Results are represented as the mean±SD from three independent experiments. n=3, ^cP<0.01 *vs* the control.

MMP-9 in a dose-dependent manner, with β-actin served as a loading control (P<0.01). Treatment with 60.0 mg/L PTF decreased MMP-2 and MMP-9 expression by 15.9% and 23.1%, respectively (Figure 6B). Furthermore, we identified a similar decreasing tendency for MMP-2 and MMP-9 in the cytoplasm after the PTF treatments via immunofluorescence staining (Figure 7).

Taken together, these findings suggested that the down-regulation of MMP-2 and MMP-9 might be involved in the inhibition of the invasion and migration of the NCI-H1703 cells after PTF treatment.

Discussion

Fructus phyllanthi, the dried ripened fruit of *Phyllanthus emblica* L, has been reported to possess a variety of potent anti-inflammatory and anti-tumor properties. The PTF is the extract prepared from fructus phyllanthi dried fruits, which contains a tannin fraction (56.8%±1.2%), including gallic acid, corilagin, ellagic acid, and chebulagic acid, as previously described[17]. Some constituents present in the PTF may act synergistically to provide better chemotherapeutic effects compared with a single constituent. Rather than the individual constituents, the PTF has been identified as an anti-tumor agent against some types of cancer *in vivo*. Our previous studies have demonstrated that treatment with PTF (2 g/kg) reduces tumor weights in tumor bearing mice, especially in Lewis lung cancer-implanted C57 mice. The current study was designed to examine the effects of the PTF on lung cancer cell metastasis and its underlying molecular mechanism *in vitro*.

Several cancer cell lines, including HT1080, NCI-H460, NCI-H1703, A549, HepG2, HGC-27, SK-N-SH, Caco-2, A498, and MCF-7, have been used to screen the cell cytotoxicities of PTF 48 h after administration. Our results indicated that the human lung squamous carcinoma cell NCI-H1703 (IC_{50}=33.0 mg/L) exhibited increased susceptibility to the PTF compared with the other cells with a 48-h exposure.

This study demonstrated that the PTF could exert potent anti-tumor activities, including the inhibition of proliferation and the induction of apoptosis. It also exerted concentration-dependent inhibitory effects on the migration and invasion of NCI-H1703 and HT1080 cells in the absence of cytotoxicity.

The induction of apoptosis is considered to be one potential mechanism of cancer development inhibition, and many types of tannin agents, such as proanthocyanidins[18] and casuarinin[19], have been shown to act through the induction of apoptosis to inhibit the lung cancer process. Apoptosis may represent a protective mechanism against neoplastic development via the removal of genetically damaged cells or cells that have improperly proliferated. In this study, we used a flow cytometry to identify the effects of PTF on the induction of apoptosis in NCI-H1703 cells and found that it induced apop-

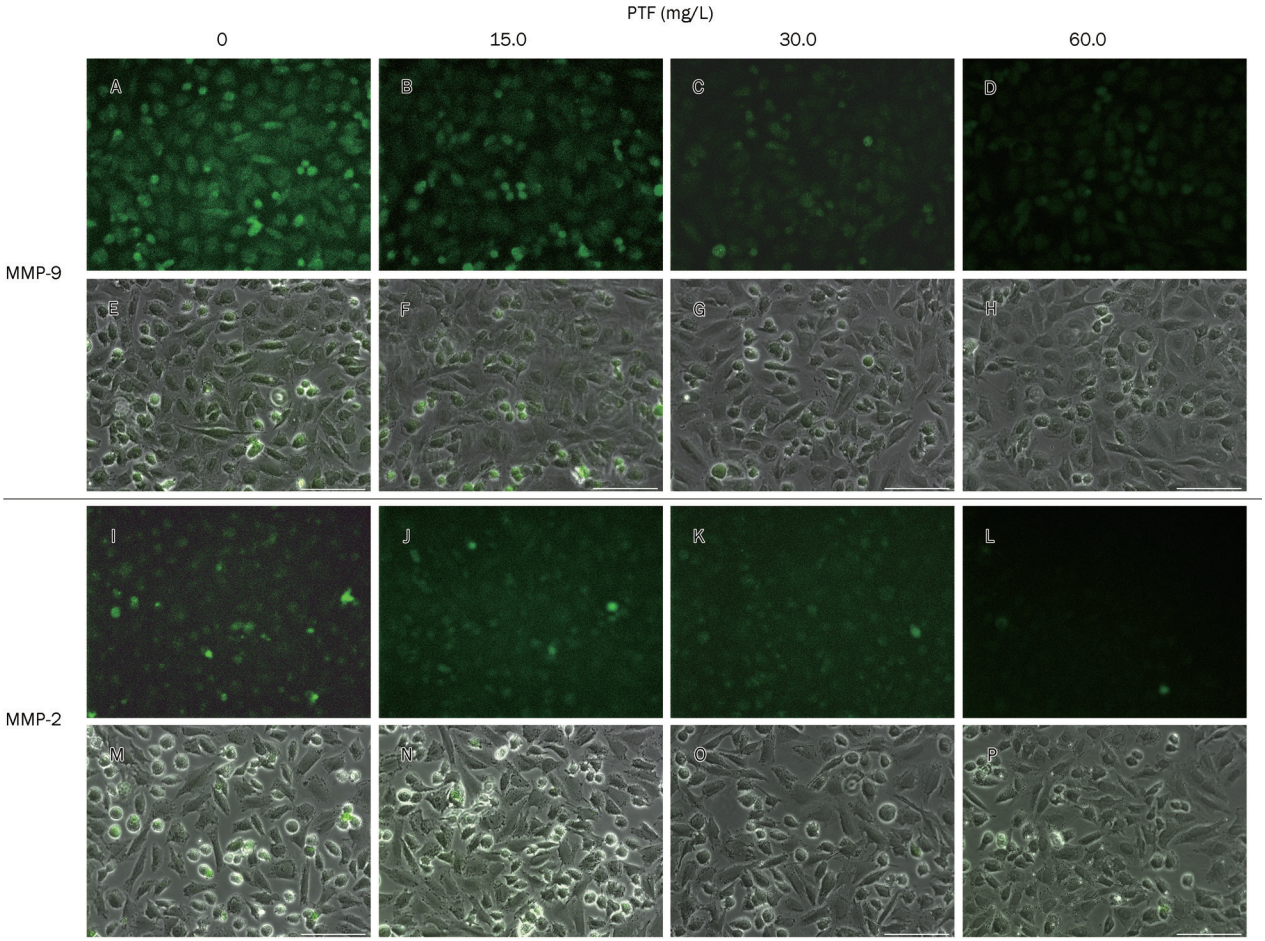

Figure 7. Fluorescence images of MMP-2 and MMP-9 expression in NCI-H1703 cells treated with PTF. (A–D) MMP-9 stain shows the responses to 0, 15.0, 30.0, and 60.0 mg/L PTF treatments, respectively. (E–H) Images A–D with a bright field overlay, respectively. (I–L) MMP-2 stain shows the responses to 0, 15.0, 30.0, and 60.0 mg/L PTF treatments, respectively. (M–P) Images I–L with a bright field overlay, respectively. A 100 μm scale bar is shown.

tosis in a dose-dependent manner, especially during early apoptosis.

Distant metastasis in lung cancer is a common occurrence in malignant tumors. Clinical statistics have demonstrated that more than 80% of cancer patients die of tumor invasion and metastasis, which are the most dangerous stages in tumor progression processes[20]. The metastatic cascade is a complex, multistage process involving the modulation of the cell phenotype, detachment and migration from the primary tumor, invasion through the extracellular matrix or basement membrane, and attachment to the remote tissues[4, 21]. Therefore, the inhibition of tumor metastasis represents a key target for cancer treatment. In this study, we used a migration and transwell chamber invasion assays to identify the effects of the PTF on the migration and invasion abilities of NCI-H1703 cells. Compared with the control group, 7.5 mg/L of the PTF, which was a non-cytotoxic concentration, significantly inhibited the migration and invasion of the NCI-H1703 cell in a time-dependent manner. We subsequently selected highly metastatic human fibrosarcoma cells (HT1080) to confirm the anti-migration and ainti-invasion effects of the PTF in the absence of a cytotoxic concentration at 25.0, 50.0 or 100.0 mg/L. The results indicated that the PTF significantly reduced the migration area of HT1080 cells and the number of cells that crossed the Matrigel in a time- and dose-dependent manner. These results suggested that the anti-tumor effect of the PTF might be associated with the inhibition of tumor invasion and metastasis.

Although the anticancer activities of the PTF have been well established, the detailed underlying molecular mechanism remains unclear. In this study, we used Western blotting and immunofluorescence staining to elucidate the molecular and biological pathways activated or inhibited by the PTF.

MAPK pathways mediate a wide variety of cellular behaviors. Its main subgroups, the ERK and JNK MAPK kinases, have been implicated in a wide range of complex biologic processes, such as cell proliferation, differentiation, death, migration, and invasion. MAPK pathways play an important role in lung cancer apoptosis[22]. In general, ERK and JNK MAP kinases are present in their non-activated forms in the

cytoplasm. *In vitro* studies have demonstrated that oxidative stress, inflammatory cytokines, and other factors can activate the JNK and ERK MAPK pathway, in which JNK activation can promote apoptosis, whereas ERK activation leads to anti-apoptotic effects[23, 24]. Thus, we investigated the effects of the PTF on the expression of MAPK pathways, including the total and phosphorylated ERK1/2 and JNK, using Western blot analysis. The results indicated that following exposure to increasing concentrations of the PTF, the level of phosphor-ERK1/2 was down-regulated and the level of phosphor-JNK was up-regulated. Thus, the PTF may induce tumor cell apoptosis through the regulation of the ERK1/2 and JNK MAPK signaling pathway.

MMPs are a class of proteolytic enzymes that are closely associated with tumor invasion and metastasis. Under normal physiological conditions *in vivo*, their synthesis, secretion, and degradation activity are under strict control and regulation. However, their activities are increased during tumor invasion and metastasis which may promote these processes[25]. MMP-2 and MMP-9 are the main enzymes that degrade type IV collagen. Therefore, they play important roles in tumor metastasis[4]. Early studies have demonstrated that MMP-2 and MMP-9 exhibited increased expression in lung cancer tissues[26]. In this study, we identified the effects of the PTF on MMP-2 and MMP-9 expression in NCI-H1703 cells using Western blotting and immunofluorescence. Both results demonstrated that the PTF inhibited the expressions of MMP-2 and MMP-9 in the NCI-H1703 cells compared with the control indicating that the PTF may inhibit tumor metastasis via the regulation of MMP-2 and MMP-9 expressions.

Lin *et al* has identified that the ERK-MMP-9 pathway can promote lung cancer cell invasion by stimulating the overexpression of several oncogenes[27]. The treatment of lung cancer cells with inhibitors specific to PI3K (LY 294002), ERK1/2 (PD98059), and p38 MAPK (SB203580) has been shown to decrease the MMP-2 and MMP-9 expression, demonstrating that the MAPK signaling pathway, MMP-9 and MMP-2 all play important roles in lung cancer cell migration[28]. In the present study, the PTF down-regulated phosphor-ERK and up-regulated phosphor-JNK, which appeared to cause a reduction of MMPs activity, thereby blocking the migration and invasion of the NCI-H1703 cells. Interestingly, 15 mg/L of the PTF significantly inhibited ERK activation and NCI-N1703 cell migration and invasion, but its reduction of MMP-2 and MMP-9 expression was not significant (P=0.058 and 0.061, respectively). Accordingly, we speculated that other molecular targets, such as other MMPs, may be involved in this anti-metastasis mechanism that requires further investigation[29–31].

Taken together, the significant findings of this study include the following: the PTF may induce tumor cell apoptosis by regulating the ERK1/2 and JNK MAPK signaling pathway. Furthermore, treatment of NCI-H1703 cells with the PTF inhibits cell migration and invasion in the absence of cytotoxicity, which may be associated with the inhibition of MMP-2 and MMP-9 expression via the MAPK pathway.

Acknowledgements

This project was supported by the National Natural Science Foundation of China (81274187 and 81274006).

Author contribution

Hai-juan ZHAO contributed to the performance of the pharmacological experiments and manuscript writing; Ting LIU, Xin MAO, Shu-xian HAN, Ri-xin LIANG, Lian-qiang HUI, and Chun-yu CAO contributed to the experimental performance and data analysis; Yun YOU contributed to the pharmacological experiment design and manuscript writing; Lanzhen ZhANG contributed to the PTF preparation and chemistry experiment design.

References

1 Gong L, Mi HJ, Zhu H, Zhou X, Yang H. P-selectin-mediated platelet activation promotes adhesion of non-small cell lung carcinoma cells on vascular endothelial cells under flow. Mol Med Rep 2012; 5: 935–42.
2 Dong J, Jin G, Wu C, Guo H, Zhou B, Lv J, *et al*. Genome-wide association study identifies a novel susceptibility locus at 12q23.1 for lung squamous cell carcinoma in han chinese. PLoS Genet 2013; 9: e1003190.
3 Kenfield SA, Wei EK, Stampfer MJ, Rosner BA, Colditz GA. Comparison of aspects of smoking among the four histological types of lung cancer. Tob Control 2008; 17: 198–204.
4 Huo XS. The expression of CD44s, CD44$_v$6, MMP-2, MMP-9, TIMP-1 and TIMP-2 and their significance in non-small cell lung cancer [dissertation]. Tianjin: Tianjin Medical University; 2006.
5 Weber GF. Why does cancer therapy lack effective anti-metastasis drugs? Cancer Lett 2013; 328: 207–11.
6 Guo K, Kang NX, Li Y, Sun L, Gan L, Cui FJ, *et al*. Regulation of HSP27 on NF-kappaB pathway activation may be involved in metastatic hepatocellular carcinoma cells apoptosis. BMC Cancer 2009; 9: 100.
7 Reddy KB, Nabha SM, Atanaskova N. Role of MAP kinase in tumor progression and invasion. Cancer Metastasis Rev 2003; 22: 395–403.
8 Dhillon AS, Hagan S, Rath O, Kolch W. MAP kinase signalling pathways in cancer. Oncogene 2007; 26: 3279–90.
9 Xia Q, Xiao P, Wan L, Kong J. Ethnopharmacology of *Phyllanthus emblica* L. Zhongguo Zhong Yao Za Zhi 1997; 22: 515–8, 25, 74.
10 Weisburg JH, Schuck AG, Reiss SE, Wolf BJ, Fertel SR, Zuckerbraun HL, *et al*. Ellagic acid, a dietary polyphenol, selectively cytotoxic to HSC-2 oral carcinoma cells. Anticancer Res 2013; 33: 1829–36.
11 Lipińska L, Klewicka E, Sójka M. The structure, occurrence and biological activity of ellagitannins: a general review. Acta Sci Pol Technol Aliment 2014; 13: 289–99.
12 Yahayo W, Supabphol A, Supabphol R. Suppression of human fibrosarcoma cell metastasis by *Phyllanthus emblica* extract *in vitro*. Asian Pac J Cancer Prev 2013; 14: 6863–7.
13 Hu JF. Inhibitory effects of *Phyllanthus emblica* juice on formation of N-nitrosomorpholine *in vitro* and N-nitrosoproline in rat and human. Zhonghua Yu Fang Yi Xue Za Zhi 1990; 24: 132–5.
14 Huang QS, Lin YZ, Li HZ, Chen WQ, Qiu SL. Study on antimutangenic and antineoplastic effect of *Phyllanthus emblica* L. J Pract Med Techn 2007; 14: 3456–7.
15 Sun XF, Zhang HY, Xia Q, Zhao HJ, Wu LF, Zhang LZ, *et al*. HPLC-fingerprint-based quality evaluation on a Tibetan medicine *Phyllanthus emblica* and its tannin parts. Zhongguo Zhong Yao Za Zhi 2014; 39:

1173–8.

16 Ishizawa K, Izawa-Ishizawa Y, Ohnishi S, Motobayashi Y, Kawazoe K, Hamano S, *et al*. Quercetin glucuronide inhibits cell migration and proliferation by platelet-derived growth factor in vascular smooth muscle cells. J Pharmacol Sci 2009; 109: 257–64.

17 Wu LF. Study on Tannin fraction from *Phyllanthus Emblica* L *in vivo* [dissertation]. Beijing: Beijing University of Chinese Medicine; 2014.

18 Singh T, Sharma SD, Katiyar SK. Grape proanthocyanidins induce apoptosis by loss of mitochondrial membrane potential of human non-small cell lung cancer cells *in vitro* and *in vivo*. PLoS One 2011; 6: e27444.

19 Kuo PL, Hsu YL, Lin TC, Chang JK, Lin CC. Induction of cell cycle arrest and apoptosis in human non-small cell lung cancer A549 cells by casuarinin from the bark of Terminalia arjuna Linn. Anticancer Drugs 2005; 16: 409–15.

20 Liu J, Yang Q, Wang MZ, W, G YJ. Matrix metalloproteinases and metastasis of lung cancer. Modern Prevent Med 2003; 30: 689–93.

21 Polacheck WJ, Zervantonakis IK, Kamm RD. Tumor cell migration in complex microenvironments. Cell Mol Life Sci 2013; 70: 1335–56.

22 Doddareddy MR, Rawling T, Ammit AJ. Targeting mitogen-activated protein kinase phosphatase-1 (MKP-1): structure-based design of MKP-1 inhibitors and upregulators. Curr Med Chem 2012; 19: 163–73.

23 Smith WE, Kane AV, Campbell ST, Acheson DW, Cochran BH, Thorpe CM. Shiga toxin 1 triggers a ribotoxic stress response leading to p38 and JNK activation and induction of apoptosis in intestinal epithelial cells. Infect Immun 2003; 71: 1497–504.

24 Zhan YH, Sun M , Liu J , Liu YP, Qu XJ, Hou KZ, *et al*. Role of ERK signaling pathway in β-elemene-induced apoptosis in human renal cell carcinoma cells. Chin J Cancer Prev Treat 2012; 19: 321–3.

25 Zhen YS. Anticancer drug research and developments. 1st ed. Beijing: Chemical Industry Press; 2004.

26 Wang WX, Chen SX, Wen JF, Xiao GM, Zhou SL. Expression and metastasis prognosis of CD44V6 MMP2, MMP9, TIMP1 and TIMP2 in non-small cell lung cancer. Chin Med Engineer 2007; 15: 122–5.

27 Lin F, Chengyao X, Qingchang L, Qianze D, Enhua W, Yan W. CRKL promotes lung cancer cell invasion through ERK-MMP9 pathway. Mol Carcinog 2014. doi: 10.1002/mc.22148.

28 Chen YY, Liu FC, Chou PY, Chien YC, Chang WS, Huang GJ, *et al*. Ethanol extracts of fruiting bodies of Antrodia cinnamomea suppress CL1-5 human lung adenocarcinoma cells migration by inhibiting matrix metalloproteinase-2/9 through ERK, JNK, p38, and PI3K/Akt signaling pathways. Evid Based Complement Alternat Med 2012; 2012: 378415.

29 Weiss MB, Abel EV, Mayberry MM, Basile KJ, Berger AC, Aplin AE. TWIST1 is an ERK1/2 effector that promotes invasion and regulates MMP-1 expression in human melanoma cells. Cancer Res 2012; 72: 6382–92.

30 Tsai HC, Su HL, Huang CY, Fong YC, Hsu CJ, Tang CH. CTGF increases matrix metalloproteinases expression and subsequently promotes tumor metastasis in human osteosarcoma through down-regulating miR-519d. Oncotarget 2014; 5: 3800–12.

31 Wang JR, Li XH, Gao XJ, An SC, Liu H, Liang J, *et al*. Expression of MMP-13 is associated with invasion and metastasis of papillary thyroid carcinoma. Eur Rev Med Pharmacol Sci 2013; 17: 427–35.